International Journal of Nanoelectronics and Materials
Volume 11, No. 1, Jan 2018 [1-14]

DFT Study of the Alkali Metal Influence on Structure and Optical Properties of B_{12} Nanocluster

Fatemeh Tahmaszadeh[1] and Hamid Reza Shamlouei[1,*]

[1] *Department of Chemistry, Lorestan University, Khorram Abad, Iran*

Received 14 Feb 2017; Revised 6 June 2017; Accepted 17 July 2017

ABSTRACT

Boron with electron deficiency has the tendency in auto-combining to form polyhedral structures. The icosahedral form of B_{12} is the structural block of boron clusters which undergo exothermic dimerization reaction. It was found that the annular shape of B_{12} was more stable in comparison with icosahedral B_{12}. Structural and optical properties of the icosahedral form and annular shape of B_{12} were modified by alkali metal atoms on their surface and it was demonstrated that the reaction of alkali metal atoms with IS-B_{12} is exothermic due to its instability. Additionally the alkali metal has greater effect on the optical properties of icosahedral form of B_{12} nanocluster. As the result, the higher polarizability was obtained for K@IS-B_{12} nanocluster (269.2 and 399.2 a.u. for mono and di K atom respectively). The modification in first hyperpolarizability for mono-alkali metal atoms on IS-B_{12} surface was more considerable than di-alkali metal atom. On the other hand, di-alkali metal atom has slight effect on first hyperpolarizability. The maximum first hyperpolarizability obtained for mono K atom attached to IS-B_{12} nanocluster (about 22500 a.u.).

Keywords: Icosahedral B_{12}, NLO, first hyperpolarizability, alkali metal, PACS's No: 42.65.–k, 42.70.Nq, 42.70.Mp

1. INTRODUCTION

Compounds with high nonlinear optical properties have great potentials in the fields of optoelectronic and photonic devices, especially the generation of optical harmonics. These great applications have attracted scientists to investigate the material with high non-linear optical (NLO) properties [1-7]. In science and technology, there are many effective agents for enhancing the NLO properties in original molecule such as electron donor and recipient groups, establishment of π electron, and doping atom [8-11]. Alkali metal attachment [12-13], transition metal doping [14] and alkali metal superoxide adsorption [15-16] on nanoclusters are among the factors responsible for high NLO properties. After exploration of carbon nanotubes by Iijima [17] and observation of the carbon nanotubes unique properties [18-20], scientists begin to study the new nano-scale material. Among the nano-scale materials, the cages of inorganic compound had special properties which was synthetized and detected. For instance, the boron nitride clusters, have unique properties. One of the properties is the auto-combining with itself to form polyhedral structures which is one of the most interesting properties of boron with electron deficiency. The polyhedral form is known as Icosahedron form where twelve atoms occupy twelve vertices. While their dimensions of 5.1Å are considerably larger than single atoms, the B_{12} polyhedron groups act as single units to form three dimensional boron clusters [21]. So it is clear that the icosahedron form of B_{12} play an unquestionable role in bulk

* Corresponding author: Physical Chemistry Group, Chemistry Department, Lorestan University, Khorram Abad, Iran. Tel fax: +98-6633120618. Email address: shamlouei.ha@lu.ac.ir

properties of boron. Electron deficiency of this molecule makes it suitable to undergo various reactions with other atoms. For instance, boron can combines with some rare earth elements such as Lu, Y, Yb to form LuB_{12}, YB_{12} and YbB_{12} respectively [22]. Additionally, boron can combine with aluminium and carbon to form AlB_{12} [23] and $B_{12}C_3$ [21] respectively. In addition, boron is also used as high-dose ion implantation of dopant atoms into silicon [24-25]. In this research, the B_{12} structure was employed to study its properties and the effect of alkali metal doping on B_{12} structure and optical properties by using the density functional theory (DFT) method. DFT is among the most extensive and useful methods available in condensed-matter physics, computational physics, and computational chemistry. In this theory, the properties of a many-electron system can be determined by using function of electron density. When taken the exchange and correlation interactions into consideration, the DFT method has advantage from the Hartree–Fock method.

2. COMPUTATIONAL DETAILS

The optimized geometrical structures of annular form of B_{12} (RS-B_{12}), icosahedron form of B_{12} (IS-B_{12}) and the combination of annular form and icosahedron form with alkali metal atoms were calculated using density functional methods at B3LYP/6-311+G(d) level of theory. The nature of the stationary points was proven using the frequency analysis at the same computational level. The frequency analysis was performed to calculate the enthalpy of Gibbs free energy. The spin-unrestricted approach was applied to describe the geometry optimization, electronic structure and NLO properties of all structures. The new density functional Coulomb-attenuated hybrid exchange-correlation functional (CAM-B3LYP) which is suitable to predict the molecular NLO properties of a large system [26-27] was employed to calculate the polarizability and first hyperpolarizability of nanoclusters. All calculations were performed using Gaussian 09 package [28].

The highest occupied molecular orbital energy and the lowest unoccupied molecular orbital energy (HOMO-LUMO) gap (E_g) values are used in order to explore the electronic properties of the considered clusters. The HOMO-LUMO gap has the following operational equation:

$$E_g = \varepsilon_H - \varepsilon_L \tag{1}$$

where ε_H and ε_L is the highest occupied molecular orbital (HOMO) and the lowest unoccupied molecular orbital (LUMO) energies respectively.

Variation of the energy with the electric field strength is given by:

$$\frac{dE}{d\varepsilon} = -\langle \mu_z \rangle \tag{2}$$

In presence of the electric field (ε), the energy of molecule (E) can be considered as Taylor expansion relative to its energy in the absence of the field E(0):

$$E = E(0) + \left(\frac{dE}{d\varepsilon}\right)_0 \varepsilon^2 + \frac{1}{2!}\left(\frac{d^2E}{d\varepsilon^2}\right)_0 \varepsilon^2 + \frac{1}{3!}\left(\frac{d^3E}{d\varepsilon^3}\right)_0 \varepsilon^3 + \cdots \tag{3}$$

where the subscript 0 indicates that the derivative is evaluated at ε =0. When the Eq. (3) mixed to Eq. (2), the following result is obtained.

$$\langle \mu_z \rangle = -\left(\frac{dE}{d\varepsilon}\right) - \left(\frac{d^2E}{d\varepsilon^2}\right)\varepsilon - \frac{1}{2}\left(\frac{d^3E}{d\varepsilon^3}\right)\varepsilon^2 + \cdots \tag{4}$$

The expectation value of the electric dipole moment in the presence of the electric field is the sum of a permanent dipole moment and the contributions induced by the field. Therefore, the expectation value of the electric dipole moment in the presence of the electric field can be written as shown in Eq. (5):

$$\langle \mu_z \rangle = \mu_{0z} + \alpha_{zz}\varepsilon + \frac{1}{2}\beta_{zzz}\varepsilon^2 + \cdots \quad (5)$$

If the expectation value of μ in all directions was requested, the following equation can be used.

$$\langle \mu \rangle = \boldsymbol{\mu} + \boldsymbol{\alpha}.\varepsilon + \frac{1}{2}\boldsymbol{\beta}\varepsilon^2 + \cdots \quad (6)$$

where $\boldsymbol{\mu}$ is the μ_x, μ_y, and μ_z, $\boldsymbol{\alpha}$ and $\boldsymbol{\beta}$ are the matrix elements of polarizability and first hyperpolarizability. The simplest polarizability (α), characterizes the ability of an electric field to distort the electronic distribution of a molecule related to linear optical properties. Higher order polarizabilities (hyperpolarizabilities β, γ, etc.) describe the nonlinear response of atoms and molecules related to a wide range of phenomena from nonlinear optics [29-31].

Using two-level model [32], the relation between hyperpolarizibility and other time dependent properties were obtained through the following relation:

$$\beta \propto f\Delta\mu/\Delta E^3 \quad (7)$$

where ΔE represent the transition energy, f represent the oscillator strength, and Δμ indicate the difference in the dipole moments between the ground state and the crucial excited state. In this model, β is proportional to ΔE^3 hence ΔE is the decisive factor in the first hyperpolarizability [33].

Due to the dependency of the first hyperpolarizability on ground and excited state properties, the time-dependent density functional theory (TD-DFT) calculations at CAM- B3LYP/6-31+G(d) level of theory were done to obtain the excitation energy and the differences of their dipole moments between the ground state and excited state as well as the oscillator strength *f*.

3. RESULTS AND DISCUSSION

3.1 Optimized structure

The chemical bond between the icosahedron-B_{12} plays an important role in the chemistry of boron compounds. Therefore, in order to understand the nature of, chemical bond between the icosahedron-B_{12}, firstly, the structure of IS-B_{12} was optimized at B3LYP/6-31+G(d) level of theory. Then the dimerization of IS-B_{12} and annular shape of B_{12} was investigated. The optimized structure of IS-B_{12}, dimer of B_{12} and RS-B_{12} were calculated and illustrated in Figure1 (a), Figure 1 (b) and Figure 1 (c) respectively.

In Figure 1, two types of B-B bond exist. R1 is located between two boron atoms inside each monomer and R2 is located between two boron atoms in two adjacent monomers. In Figure 1 (a), the B_{12} consists of icosahedral structure which is a polyhedron form with twenty triangular faces. As mentioned in the introduction, the B_{12} polyhedron groups act as single unit which have high tendency to play as monomer forming three dimensional boron clusters.

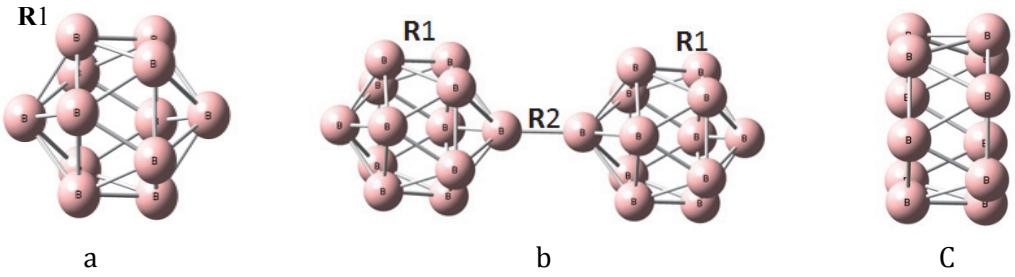

Figure 1. Optimized structures of (a) icosahedral B_{12}, (b) dimer of IS-B_{12} and (c) annular B_{12} (RS-B_{12}) at B3LYP/6-311+G

In Table 1, the structural information (R1 and R2 values) as well as the energetic properties of IS-B_{12} and its dimer was reported. The R1 in the IS-B_{12} is 1.705 which is slightly different from B-B obtained by Yamauchi et. al (1.75) [34]. As the result of combining two B_{12} molecules, the R1 bond length slightly shortened and the dimerization produced an exothermic reaction. The B-B bond length that occurred between two adjacent monomers is 1.687 which is in agreement with previous data (1.71) [34].

Table 1 The structural information, energetic properties of IS-B_{12} and its dimer

	R1	R2	ΔE (kCal.mol^{-1})	ΔH(kCal.mol^{-1})	ΔG(kCal.mol^{-1})
IS-B_{12}	1.705		-1179.26	-1162.41	-1064.63
Dimer	1.692	1.687	-2450.56	-2413.88	-2202.27

In comparison to icosahedral structure, the B_{12} may exist in annular shape (ring-shape or RS) which consists of two optimized six member rings. The optimized structure of RS-B_{12} was depicted in Figure 1 (c). The energetic properties of RS-B_{12} were calculated. Interestingly the RS-B_{12} is more stable than IS-B_{12} which 295 kJ.mol^{-1} energy difference found between two configurations. Low stability of the IS-B12 may be the reason of its tendency to combine with itself. Additionally, it seems that the electron deficiency characteristic of IS-B_{12} make it suitable to react with alkali metals. Thereby, investigation was continued with the placement of lithium, sodium and potassium atoms on the surfaces the two configurations of B_{12}. The optimized structures were calculated. The structures of the adsorbed mono and di-alkali metal atoms on the IS-B_{12} surface were depicted in Figure 2.

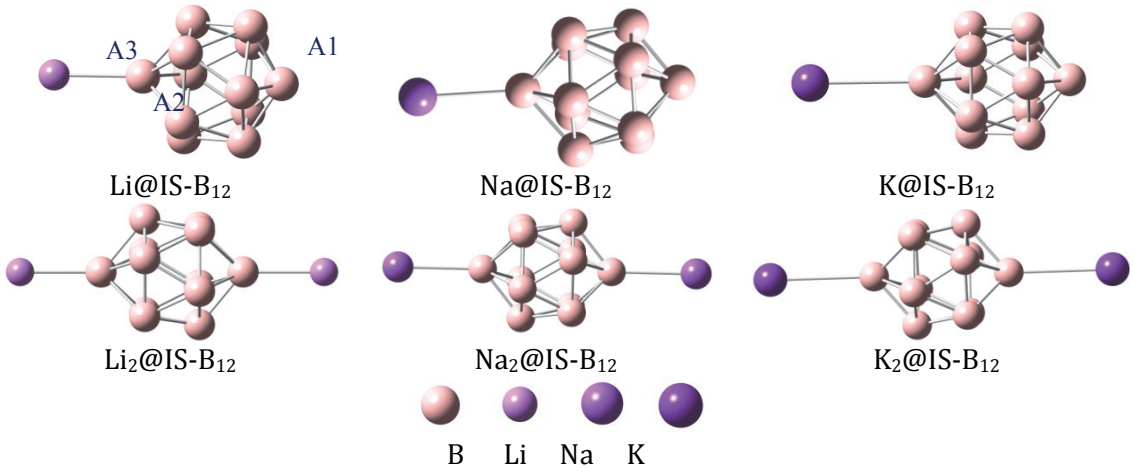

Figure 2. Optimized structures of mono and di-alkali metal adsorbed on IS-B_{12} nanoclusters at B3LYP/6-311+G(d) level of theory

As illustrated in Figure 2, four B-B and B-X (in which X correspond to alkali metal atoms) bonds exist. In Table 2, the values of A1 to A4 bond lengths for each complex of alkali metal atoms with IS-B_{12} nanocluster were compared. In the presence of lithium atoms, the A1 bond length (which is the B-B bond exist between two boron atoms far from alkali metal atoms) was shortened but in Na and K case, the A1 increases. The A2 bond length which occurs between two B near the alkali metal atoms increases in presence of alkali metal atoms. The interaction length of alkali metal atoms depend on their atomic radius and the smallest bond was obtained for lithium atom and largest for potassium atom. The interaction lengths are almost constant if the number of alkali metal atoms increase. Finally the A4 which is the distance of two boron atoms in adjacent five member rings was shortened in existence of alkali metal atoms. In continuation, the alkali metal were attached on the RS-B_{12} and their structures were optimized and depicted in Figure 3.

Table 2 The structural information of IS-B_{12} with different complexes of alkali metal

Type of structure	A1	A2	A3	A4
IS-B_{12}	1.736	-	-	1.704
Li@IS-B_{12}	1.667	1.776	2.147	1.698
Na@IS-B_{12}	1.793	1.812	2.461	1.663
K@IS-B_{12}	1.850	1.844	3.001	1.659
Li_2@IS-B_{12}	-	1.820	2.153	1.647
Na_2@IS-B_{12}	-	1.810	2.461	1.647
K_2@IS-B_{12}	-	1.876	2.918	1.663

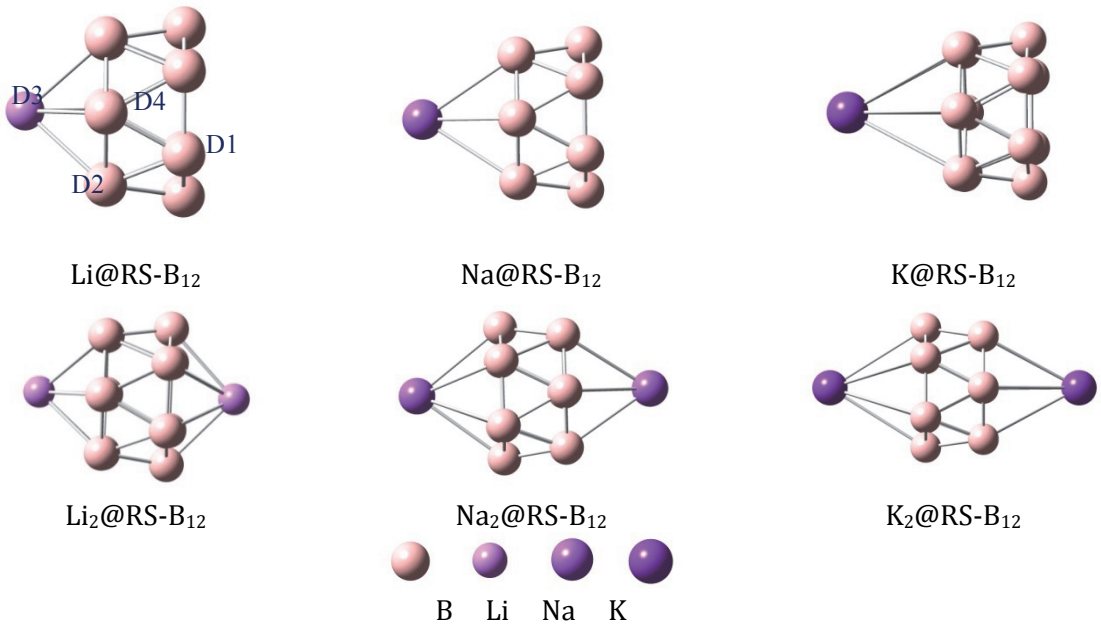

Figure 3. Optimized structures of mono and di-alkali metal atom adsorbed on annular B_{12} at B3LYP/6-311+G(d) level of theory

The information of optimized structure of mono and di-alkali metal atoms complex of RS-B_{12} was gathered in Table 3.

Table 3 The structural properties of RS-B_{12} and different complexes of alkali metal with it

Type of structure	D1	D2	D3	D4
RS-B_{12}	1.624	-	-	1.695
Li@RS-B_{12}	1.611	1.617	2.244	1.722
Na@RS-B_{12})	1.610	1.617	2.663	1.725
K@RS-B_{12}	1.609	1.616	3.070	1.727
Li_2@RS-B_{12}	-	1.605	2.225	1.743
Na_2@RS-B_{12}	-	1.605	2.641	1.750
K_2@RS-B_{12}	-	1.603	3.034	1.757

As shown in Table 3, after combination of RS-B_{12} with alkali metal atoms, the D1 and D2 bonds were shortened and the strength of them increases in presence of alkali metal atoms. When two alkali metal atoms attached to RS-B_{12} the B-B bond length was further shortened. Similar to IS-B_{12}, distance of alkali metal atoms to B atoms depend on the size of alkali metal atom and shorter distance was seen for lithium atom. When the number of lithium atoms increases, the interaction length between the atoms decreases. On the other hand, the distance between two B atoms in adjacent ring (D4) increases in presence of alkali metal atoms.

3.2 Electronic properties

For calculation the electronic properties of molecule, the HOMO and LUMO orbitals for IS-B_{12} and RS-B_{12} complex with alkali metal atoms were calculated and the energy gap values were obtained. In Figure 4 the HOMO and LUMO orbitals for all considered clusters and the corresponding density of state (DOS) was demonstrated.

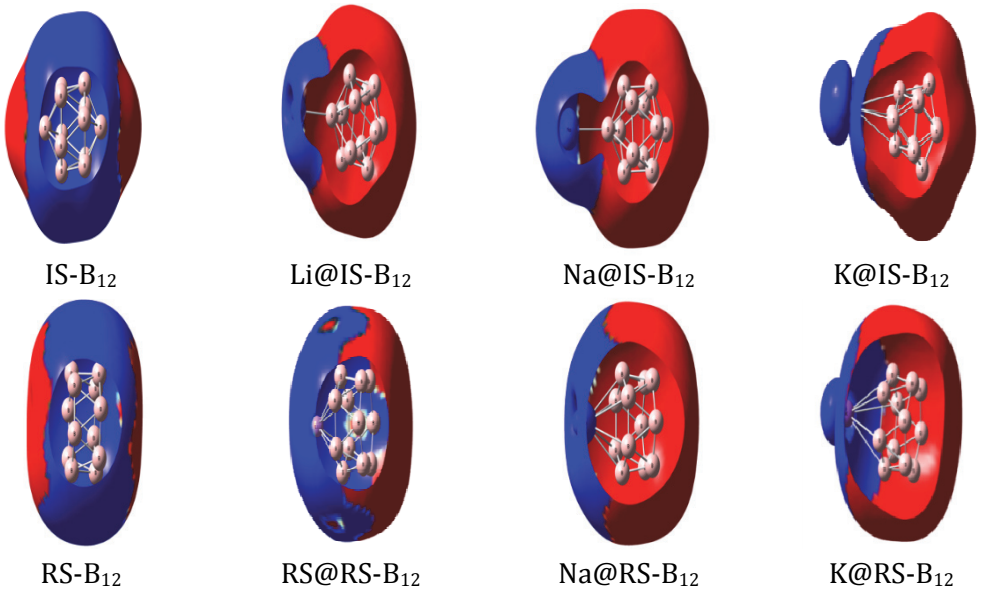

Figure 4. The HOMO, LOMO orbitals for all clusters and corresponding DOS for them

The results of the E_{HOMO}, E_{LUMO}, E_g and dipole moment (μ) for each clusters were shown in Table 4. For the pristine RS-B_{12} and IS-B_{12}, the obtained HOMO energies are -6.12 and -4.6 respectively whereas, the LUMO energies for RS-B_{12} and IS-B_{12} are -3.14 and -3.6 respectively. The E_g for RS-B_{12} and IS-B_{12} are 2.98 eV and, 1 eV respectively. The lower E_g of IS-B_{12} demonstrates the instability in its structure. Contradictory, the influence of alkali metal on E_g may be the result of difference between the E_g of two pristine B_{12} configurations. The HOMO and LUMO energies were increased by alkali atom presence. However, increase in E_{LUMO} for M@IS-B_{12} is more considerable and so the E_g increases. On the other hand, for RS-B_{12}, increasing in E_{HOMO} is more considerable and so the E_g decreases. The calculated E_{HOMO}, E_{LUMO}, E_g and electrical dipole moments for the pristine B_{12} and M@B_{12} in two configurations are shown in Table 4.

Table 4 The results of E_{HOMO}, E_{LUMO}, E_g and μ for two configurations of B_{12} and complex of alkali metal atoms with them

Type of structure	E_{HOMO}	E_{LUMO}	E_g	μ
RS-B_{12}	-6.12	-3.14	2.98	0.00
Li@RS-B_{12}	-4.51	-2.29	2.22	3.9378
Na@RS-B_{12}	-4.11	-2	2.11	7.0170
K@RS-B_{12}	-3.83	-1.76	2.07	9.813
Li_2@RS-B_{12}	-4.53	-1.98	2.55	0.0004
Na_2@RS-B_{12}	-3.82	-1.46	2.36	0.0002
K_2@RS-B_{12}	-3.34	-1.06	2.28	0.0009
IS-B_{12}	-4.6	-3.6	1	0.00
Li@IS-B_{12}	-4.57	-2.47	2.1	7.7416
Na@IS-B_{12}	-4.32	-2.68	1.64	8.0734
K@IS-B_{12}	-4.47	-2.61	1.86	11.3340
Li_2@IS-B_{12}	-3.77	-1.95	1.82	0.0015
Na_2@IS-B_{12}	-3.82	-2.08	1.74	0.0012
K_2@IS-B_{12}	-1.72	-3.04	1.32	0.0014

To indicate the orientation of the complex of alkali metal atom with two configuration of B_{12} in electric field, the molecular electrostatic potential surface of them were plotted and depicted in Figure 5. In Figure 5, the locations of the various most positive and most negative regions were shown by molecular electrostatic potential surface. In IS-B_{12} and RS-B_{12}, the electron density mainly concentrated over two head of the molecules. The distribution of charge is symmetrical and the clusters have no orientation in electric fields. In the complex of alkali metal atom with these clusters, the head of alkali metal complex have positive charge and other head has negative charge which oriented toward the positive pole. Additionally the positive charge of the alkali metal heads illustrates the charge transfer from alkali metal to nanocluster.

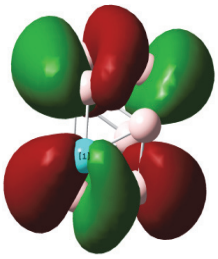

HOMO

LUMO

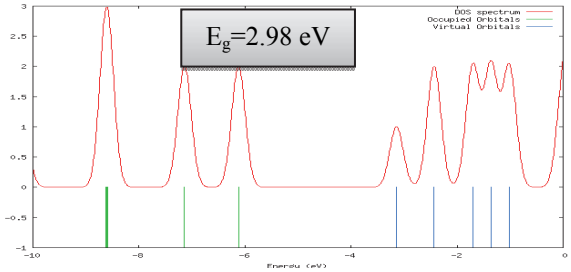

$RS\text{-}B_{12}$

HOMO

LUMO

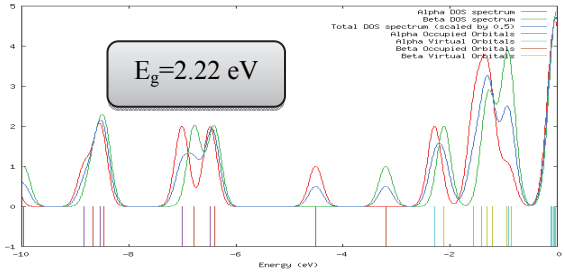

$Li@RS\text{-}B_{12}$

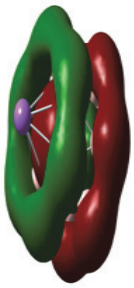

HOMO

LUMO

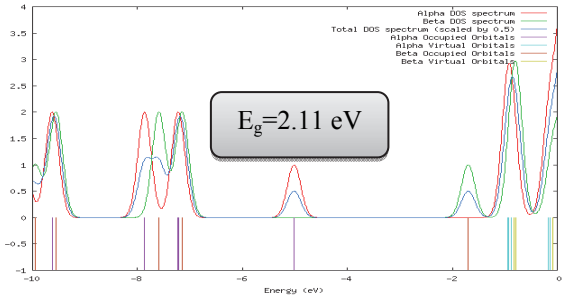

$Na@RS\text{-}B_{12}$

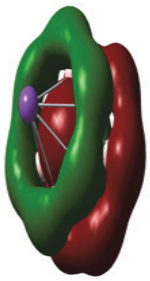

HOMO

LUMO

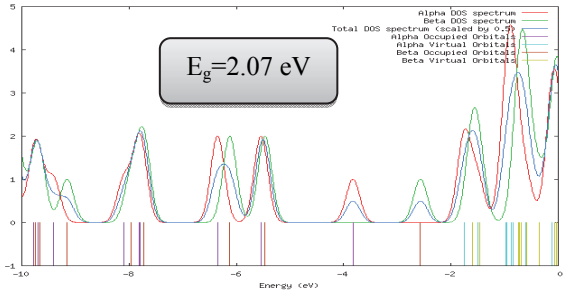

$K@RS\text{-}B_{12}$

HOMO

LUMO

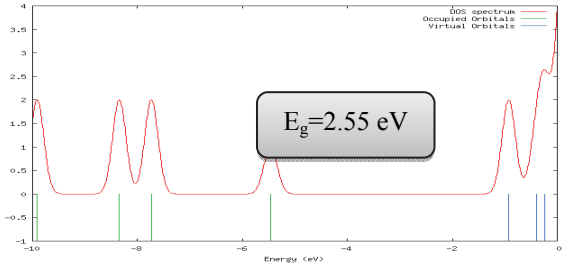

$Li_2@RS\text{-}B_{12}$

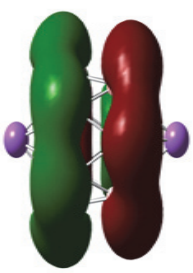

HOMO

LUMO

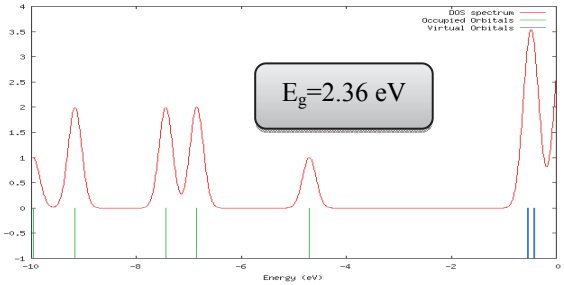

Na_2@RS-B_{12}

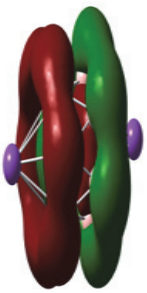

HOMO

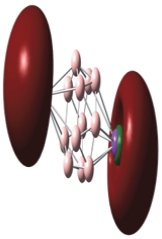

LUMO

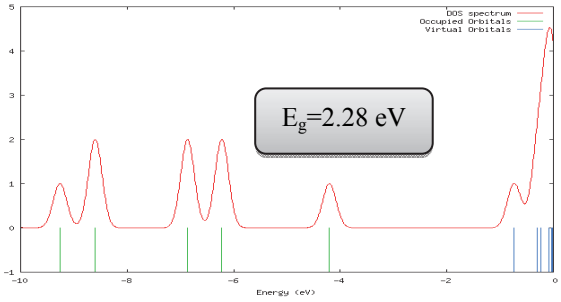

K_2@RS-B_{12}

HOMO

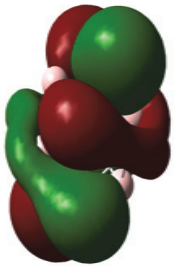

LUMO

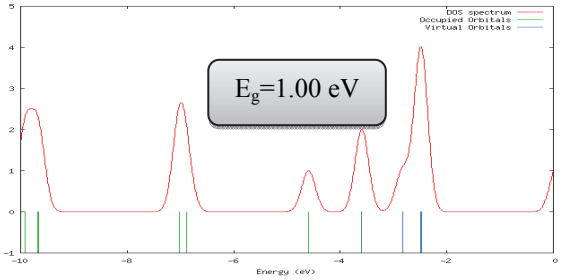

IS-B_{12}

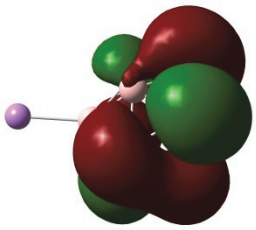

HOMO

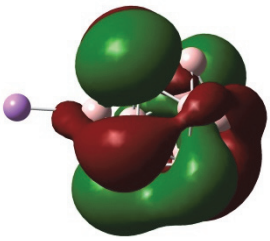

LUMO

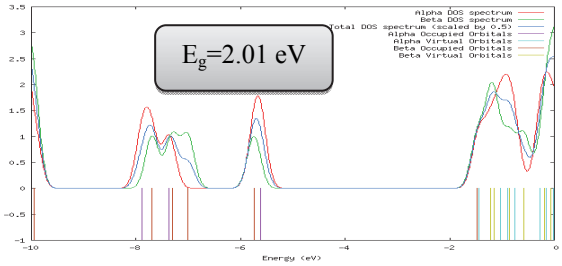

Li@IS-B_{12}

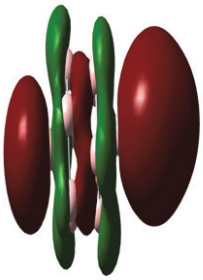

HOMO

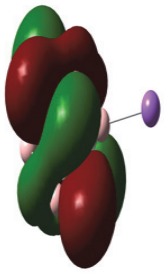

LUMO

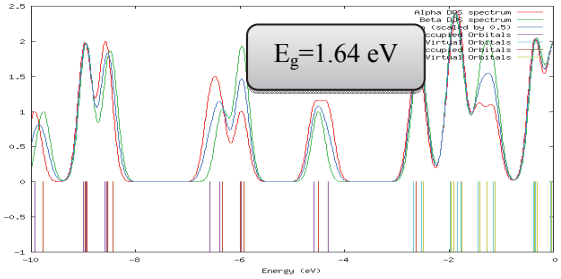

Na@IS-B_{12}

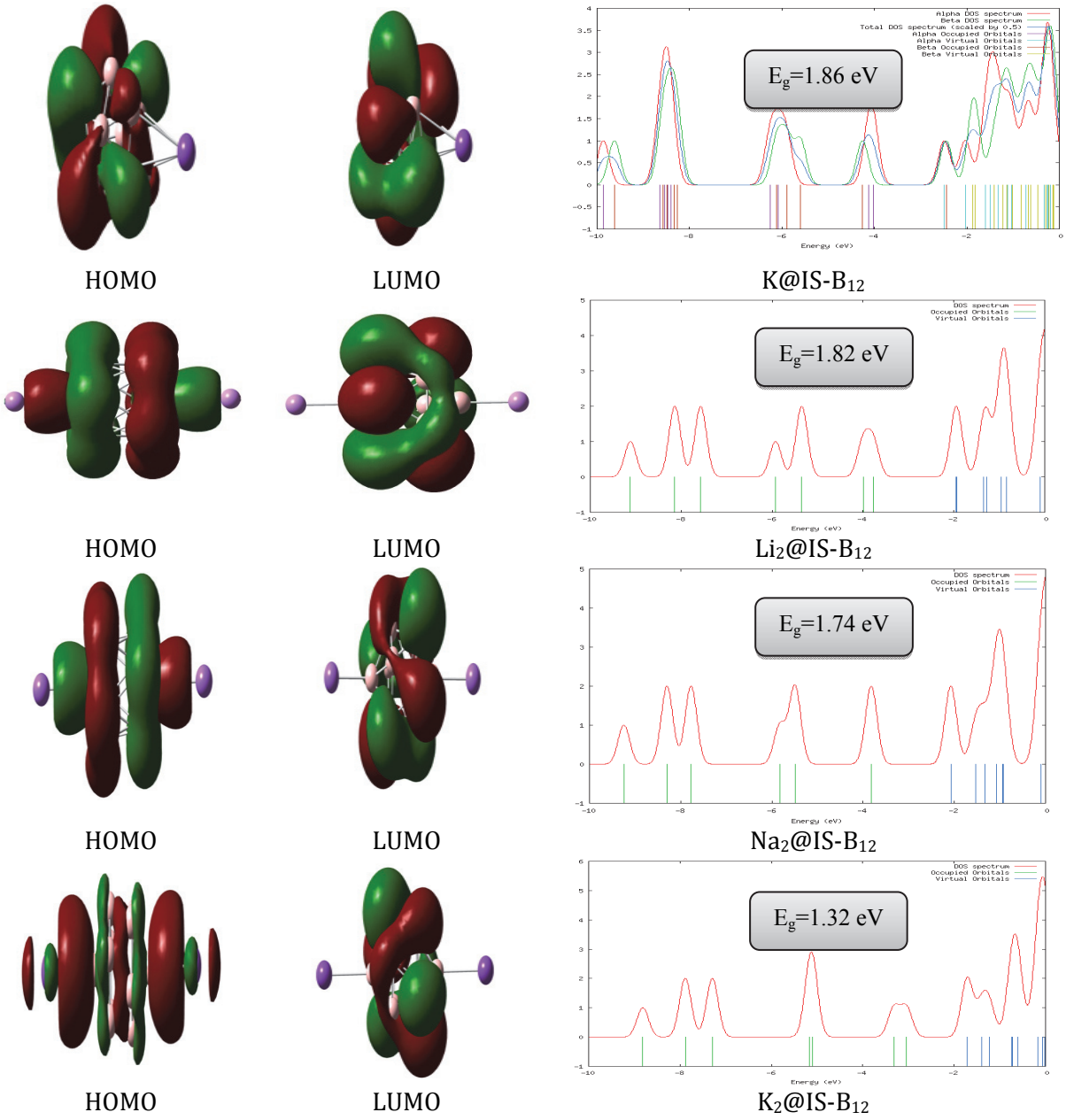

Figure 5. Molecular electrostatic potential surface of the complex of alkali metal atom with two configuration of B_{12}.

3.3 Optical properties

The polarizability (α), and first order static hyperpolarizability (β_0) of pristine B_{12} and $M@B_{12}$ in two configurations are calculated using DFT theory at CAM-B3LYP/6- 31+G (d,p) level. The values of polarizability (α), and first order static hyperpolarizability (β_0) for mentioned structures are presented in Table 5.

Table 5 Calculated results of α and β for two configurations of B_{12} and different complex with alkali metal atoms

Type of structure	α	β_o	*f*(a.u.)
RS-B_{12}	148.6	0.31	0.0003
Li@RS-B_{12}	180.2	1877.6	0.0475
Na@RS-B_{12}	194.3	5909.1	0.0528
K@RS-B_{12}	202.6	7159.3	0.0544
Li_2@RS-B_{12}	202.6	1.5	0.0982
Na_2@RS-B_{12}	243.3	0.9	0.2310
K_2@RS-B_{12}	269.2	4.4	0.2008
IS-B_{12}	192.0	0.015	0.0320
Li@IS-B_{12}	204.9	5741.7	0.0107
Na@IS-B_{12}	210.7	11333.9	0.0010
K@IS-B_{12}	230.1	22491.2	0.0054
Li_2@IS-B_{12}	231.2	1.09	0.1331
Na_2@IS-B_{12}	299.4	1.8	0.4446
K_2@IS-B_{12}	392.2	0.036	0.5889

According to data presented in Table 5, the polarizability of IS-B_{12} and RS-B_{12} is 192.0 and 148.6 respectively. The larger polarizability in IS-B_{12} is probably due to its higher volume. Alkali metal atoms attachment on both configurations of B_{12} increase it polarizability which is predictable and the order of increase in polarizability is K > Na > Li. The first hyperpolarizability for B_{12} in the two configurations (IS-B_{12} and RS-B_{12}) is near zero. Consequently, the attachment of alkali metal remarkably increased the polarization. Increase in β_0 as consequence of alkali metal presence is much considerable for IS-B_{12} configuration. Similar to polarizability, the order of β_0 improvement is K > Na > Li. Table 5 proven that it was predictable that attachment of two alkali atoms on nanocluster have no improvement effect on the hyperpolarizability (due to high degree of symmetry). In addition, the maximum of first hyperpolarizability was obtained for K@IS-B_{12} (22491.2 a.u.)

3.4 TD-DFT

The two-level model [27,28] was used to explain the increase in hyperpolarizability of B_{12} nanoclusters. This model is considered as:

$$\beta_0(two-level) \propto \frac{\Delta\mu \cdot f_0}{\Delta E3} \tag{8}$$

where ΔE, f_0 and Δμ are the transition energy, oscillator strength, and difference in the dipole moments between the ground state and the crucial excited state with the largest oscillator strength. According to Eq. (3) the β_0 value is reversely proportional to the third power of the transition energy, so it is the noteworthy factor in the first hyperpolarizability. Time-dependent density functional theory (TD-DFT) calculations at CAM-B3LYP/6-31+G(d) level of theory was used to obtain transition excited state properties. The properties such as excitation energies ΔE(eV), xcitation wavelength λ(nm) nd oscillator strengths *f(a.u)* of all configurations listed in Table 6.

Table 6 The excitation energy ΔE, wavelength λ and oscillator strength *f* for two configurations of B_{12} nanocluster

Type of structure	ΔE (eV)	λ(nm)	*f(a.u.)*
RS-B_{12}	2.8738	431.43	0.0003
Li@RS-B_{12}	2.1721	570.79	0.0475
Na@RS-B_{12}	2.0711	598.63	0.0528
K@RS-B_{12}	2.0474	605.58	0.0544
Li_2@RS-B_{12}	2.6880	461.26	0.0982
Na_2@RS-B_{12}	2.3241	533.47	0.2310
K_2@RS-B_{12}	2.0924	592.55	0.2008
IS-B_{12}	1.1727	1057.26	0.0320
Li@IS-B_{12}	1.2472	994.09	0.0107
Na@IS-B_{12}	1.1845	1046.75	0.0010
K@IS-B_{12}	1.0891	1138.42	0.0054
Li_2@IS-B_{12}	2.1930	565.37	0.1331
Na_2@IS-B_{12}	2.2450	552.26	0.4446
K_2@IS-B_{12}	1.7241	719.12	0.5889

Results in Table 6 is in agreement with Eq. (3). For similar configurations, the first hyperpolarizability has the same behaviour as the reverse transition energy. The first hyperpolarizibility (β_0) for the same structures with one adsorbed alkali metal atoms were plotted as function of transition energy (ΔE) and illustrated in Figure 6.

In Figure 6, it is clear that the excitation energy inversely related to the values of first hyperpolarizibility. Small changes in transition energy can cause drastic modifications in first hyperpolarizability. Among the M@IS-B_{12}complexes, the K@IS-B_{12} has the smallest transition energy and has large value of first hyperpolarizability (22491.2 a.u). Similarly, among the M@RS-B_{12} complexes, the K@RS-B_{12} has minimum transition energy and maximum value of first hyperpolarizability (7159.3 a.u.).

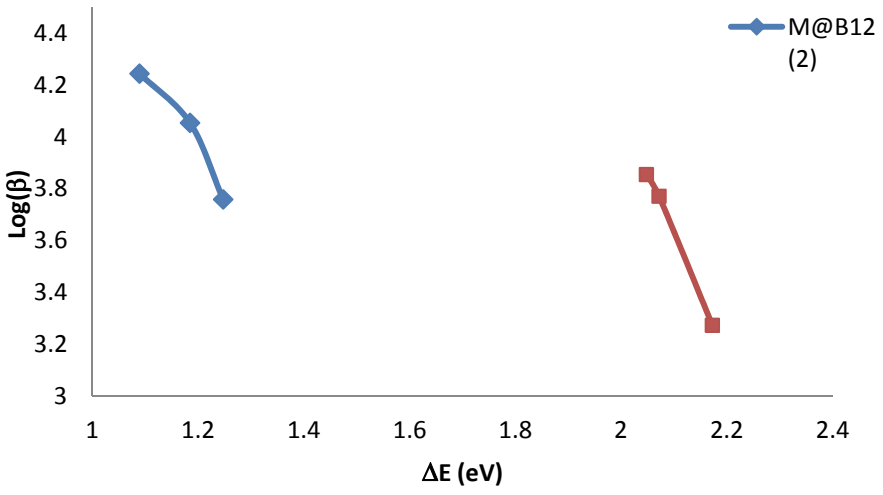

Figure 6. The logarithm of β_0 as function of transition state of two configurations of B_{12} with alkali metal atoms

4. CONCLUSION

In this research the icosahedral form of B_{12} which is the structural block of boron clusters was employed. An exothermic dimerization reaction was observed between two IS-B_{12} nanoclusters. Additionally, it was shown that the annular form of RS-B_{12} has more stability. Then, the effect of alkali metal atom on structure and optical properties of two configuration of B_{12} were explored. It was shown that the net charge transfer take place from alkali metal atom to B_{12} nanocluster. Additionally, it was discovered that the alkali metal has superior effect on the icosahedral form of B_{12} nanocluster. For instance, the higher polarizability was obtained for icosahedral in which the K atom attached to IS-B_{12} nanocluster (269.2 and 399.2 a.u. for mono and di K atom). The first hyperpolarizability for IS-B_{12} was modified by adsorption of mono-alkali metal atoms on its surface. The di-alkali metal atom on the other hand has little effect on first hyperpolarizability. The maximum first hyperpolarizability obtained for mono K atom attached to IS-B_{12} nanocluster. According to two-level model, slight reduction in transition energy significantly modifies the first hyperpolarizability which explains the alkali metal effect on first hyperpolarizability.

REFERENCES

[1] Kleinman, D. A, *Phys. Rev*. **126 (**1962) 1977
[2] Pandey. V, Mehta. N, Tripathi. S. K, Kumar. A, *J. Optelectron. Adv. M*. **7** (2005) 2641
[3] Zhong, R. L, Xu. H. L, Muhammad. S, Zhang. J, Su. Z. M, *J. Mater. Chem.* **22** (2012) 2196
[4] Tu. C, Yu. G, Yang. G, Zhao. X, Chen. W, Li. S, Huang. X, *Chem. Chem. Phys.* **16** (2014) 1597
[5] Zhou. F, He. J. H, Liu. Q, Gu. P. Y, Li. H, Xu. G. Q, Lu. J, M, *J. Mater. Chem*, **100** (2014) 6850
[6] Hatua. K, Nandi. P. K, *J. Phys. Chem. A.* **117** (2013) 12581
[7] Muhammad. S, Xu. H, Su. Z, *J. Phys. Chem. A.* **115** (2011) 923
[8] Marder. S. R, Gorman. C. B, Meyers. F, Perry. J. W, Bourhill. G, Brédas. J. L, Pierce. B. M, *Science*. **265** (1994) 632
[9] Shakerzadeh. E, *J. Inorg. Organomet. Polym*. **24** (2014) 694
[10] Shakerzadeh. E, *J. Mater. Sci.* **25** (2014) 4193
[11] Niu. M, Yu. G, Yang. G, Chen. W, Zhao. X, Huang. X, *Inorg. Chem.* **53** (2014) 349
[12] Shakerzdeh. E, Tahmasebi. E, Shamlouei. H. R , *Synth. Met.* **204** (2015) 17
[13] Shakerzdeh. E, Biglari. Z. Tahmasebi. E, *Chem. Phys. Lett.* **654** (2016) 76
[14] Shamlouei. H. R, Nouri. A, Mohammadi. A, Dadkhah. Tehrani. A, Physica. E. **77** (2016) 48
[15] Mohammadi. Hesari. A, Shamlouei. H. R, Raoof. Toosi. A, *J. Mol. Model.* **22** (2016) 189
[16] Raoof. Toosi. A, Shamlouei. H. R, Mohammadi. Hesari. A, *Chin. Phys. B.* **25** (2016) 094220
[17] Iijima. S, *Nature.* **354** (1991) 56
[18] Harris. P. F, *Carbon Nanotubes and Related Structures : New Materials for the Twenty-first Century* .Cambridge University Press (1999).
[19] Saito. R, Dresselhaus. G, Dresselhaus. M. S, *Physical Properties of Carbon Nanotubes* .Imperial College Press (1998).
[20] Dresselhaus. M. S, Dresselhaus. G, Eklund. P. C, *Science of Fullerenes and Carbon Nanotubes : Their Properties and Applications* .Academic Press (1996).
[21] Bullett. D. W, *J. Phys. C.* **15** (1982) 415
[22] Hein. H, Koeppel. C, Vetter. U, Warkentin. E, *Sc, Y, La-Lu. Rare Earth Elements: Compounds with Boron: Gmelin Handbook of Inorganic and Organometallic Chemistry* ,Springer-Verlag Berlin Heidelberg (1989).
[23] Higashi. I, *J. Solid. State. Chem.* **154** (2000) 168
[24] Mizushima. I, Watanabe. M, Murakoshi. A, Hotta. M, Kashiwagi. M, Yoshiki. M, *Appl. Phys. Lett.* **63** (1993) 373
[25] Mizushima. I, Murakoshi. A, Watanabe. M, Yoshiki. M, Hotta. M, Kashiwagi. M, *Jpn. J. Appl. Phys.* **33** (1994) 404
[26] Yanai. T, Tew. D. P, Handy. N. C, *Chem. Phys. Lett.* **393** (2004) 51

[27] Jacquemin. D, Perpète. E. A, Scalmani. G, Frisch. M. J, Kobayashi. R, Adamo. C, *J. Chem. Phys.* **126** (2007) 144105
[28] Frisch. M. J; et al., *Gaussian 09, revision 09. A0* Gaussian. Inc. Wallingford, CT (2009).
[29] Buckingham, A. D, *Adv. Chem. Phys.***12** (1967) 107
[30] McLean. A. D.,Yoshimine. M, *J. Chem. Phys.* **47** (1967) 1927
[31] Atkins P., Friedman R. Molecular Quantum Mechanics, Oxford University Press, 4th Edition
[32] Kanis. D. R, Ratner. M. A, Marks. T. J, *Chem. Rev.* **94** (1994) 195
[33] Ayan. D and Swapan. K. P, Chem. Soc. Rev. **35** (2006) 1305
[34] Yamauchi. J, Aoki. N, Mizushima. I, *Phys. Rev. B.* **55** (1997) 10245